Online ISSN 1848-3380, Print ISSN 0005-1144
ATKAFF 53(1), 9–19(2012)

Jiro Hirokawa

Plate-laminated Waveguide Slot Array Antennas and its Polarization Conversion Layers

DOI: 10.7305/automatika.53-1.143
UDK 621.396.677.029.65.09
IFAC 5.8.3

Original scientific paper

This paper reviews not only the characteristic of the linearly-polarized plate-laminated waveguide slot array antenna in the 60 GHz band but also conversion to circular or tilted linear polarization by adding a layer of apertures over the antenna. The linearly-polarized antenna achieves about 80% antenna efficiency and more than 32 dBi of gain is achieved over 4.8 GHz bandwidth. The measured cross-polarization level is well suppressed below -45 dB in the boresite even though the slots are wide. The circularly-polarized 16×16-element array antenna achieves the axial ratio less than 3 dB over 2.5 GHz bandwidth. In the tilted linearly polarized 16×16-element array antenna, the measured cross polarization is below -30 dB in the boreside over approximately 5 GHz bandwidth.

Key words: Plate-laminated-waveguide, Corporate-feed, Polarization, Diffusion bonding, Millimeter-wave

Antenski nizovi valovodnih otvor-antena i konverteri polarizacije izvedeni s pomoću planarnih laminata. U ovom se radu razmatraju ne samo karakteristike linearno polariziranih antenskih nizova valovodnih otvor-antena, izvedenih s pomoću planarnih laminata, već i konverteri u kružnu odnosno kosu linearnu polarizaciju dobiveni dodavanjem sloja otvora iznad antene. Za linearno polariziranu antenu postignuta je efikasnost od oko 80% i dobitak veći od 32 dBi u frevencijskom pojasu širine 4.8 GHz. Izmjerena križna polarizacija manja je od -45 dB u smjeru glavne latice iako su rabljeni antenski otvori bili poprilično široki. Za kružno polarizirani antenski niz sa 16×16 elemenata postignuti je aksijalni odnos manji od 3 dB u frekvencijskom pojasu širine 2.5 GHz. U antenskom nizu s kosom linearnom polarizacijom sa 16×16 elementa izmjerena jakost križne polarizacije manja je od -30 dB u smjeru glavne latice u frekvencijskom pojasu širine 5 GHz.

Ključne riječi: valovodi izvedeni s pomoću planarnih laminata, korporativna pobuda, polarizacija, difuzijsko spajanje, milimetarsko valno područje

1 INTRODUCTION

A hollow-waveguide slot array antenna is advantageous for a larger-size or a higher gain application since it neither suffers from dielectric nor radiation losses in comparison to microstrip line-fed array antennas [1]. On the other hand, a conventional waveguide slot array antenna was unsuitable for mass production due to the complicated three-dimensional feeding structure below the radiating waveguide array [2,3]. Also it was series-fed, which had a fundamental problem that the bandwidth was narrowed due to the long-line effect when the array size became large. To remedy this bandwidth problem, we proposed the structure of a double-layer corporate-feed waveguide slot array with constant element spacing smaller than free-space wavelength [4]. This antenna consists of a corporate feed waveguide arranged in the lower layer and 2×2-element small sub-array units in the upper layer. In general, multilayer structure cannot be fabricated easily by conventional techniques such as machining or die-casting. We adopt the diffusion bonding of laminated thin metal etched plates for the fabrication of a double-layer full-corporate-feed waveguide slot array antenna [5]. This fabrication technique has potential of being low cost in the millimeter-wave band because of high-precision (about 20 mm) etching of metal plates and a small number of etching patterns. The diffusion bonding at high temperature (about 1000 degrees) gives perfect electrical contacts among the laminated metal plates. In contrast with conventional multiple layer antennas in [3,6,7], the antenna efficiency and the bandwidth of the proposed antenna remain remarkable even in the higher frequency band of 60 GHz.

As for the circularly-polarized antenna, a grooved circular waveguide polarizer as the circularly-polarized element was reported [8, 9], however this was not suitable for planar antennas because the total length of 40 mm in the 30 GHz-band was as long as a horn antenna. A wideband and high efficiency corporate feed antenna with a low-

profile hexagonal aperture was reported in the 12 GHz-band [10], however it needed the placement of a dielectric component on each element to suppress grating lobes as the element spacing was larger than the free-space wavelength. We proposed an aperture array antenna by placing circularly-polarized elements over the plate-laminated waveguide slot array antenna [11]. As for the tilted-linearly-polarized antenna, there is a way to achieve low sidelobe characteristics without tapered aperture distribution for 45-degree polarization, that is, to use a diagonal plane of uniformly excited square array arrangement [12]. The diagonal plane has equivalently tapered excitation, and the first sidelobe level in the diagonal plane is -26.4 dB, whereas that in the plane parallel to the side is -13.2 dB. By using the diagonal plane, low sidelobe characteristics without degradation of aperture efficiency can be realized. Although 45 -degree linearly polarized array antennas were reported [13–16], their gain-bandwidth was narrow due to series feeding. Furthermore, the antennas in [14] and [16] had dielectric losses from the feeding and radiating waveguides, which led to degradation of antenna efficiency. We proposed a 45-degree linearly polarized configuration to be added as a layer composed of radiation slots inclined at 45 degrees to the arrangement directions of the elements, so that the direction of the polarization becomes parallel to the diagonal of the square array arrangement [17].

2 LINEARLY-POLARIZED ANTENNA

2.1 Structure

Fig. 1 shows the configuration of the double-layer full-corporate-feed hollow-waveguide linearly-polarized slot array antenna.

The shaded area shows the full-corporate-feed waveguide that consists of several H-plane T-junctions located in the lower layer. The antenna is fed through a feed aperture of the same size as a standard WR15 rectangular waveguide located on the back side. A coupling aperture is placed at each end of the full-corporate-feed waveguide with an offset. Radiating slots are arranged in both x and y directions with constant spacing. Fig. 2 shows the exploded perspective view of the 2×2-element subarray. The 2×2-element subarray is included into a cavity on the upper layer. The cavity is partitioned into four spaces by two sets of walls extending in the x and y directions. The coupling aperture is placed at the center of the cavity. In order to realize strong excitation of the cavity, it has an offset from the center axis of the waveguide, which gives the physical maximum for the given width of the coupling aperture and the waveguide. The 2×2-element subarray is excited in phase and with equal amplitude.

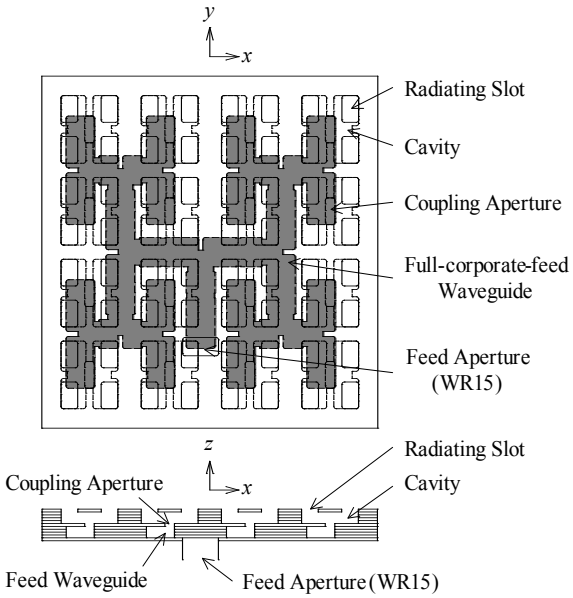

Fig. 1. Configuration of the linearly-polarized antenna

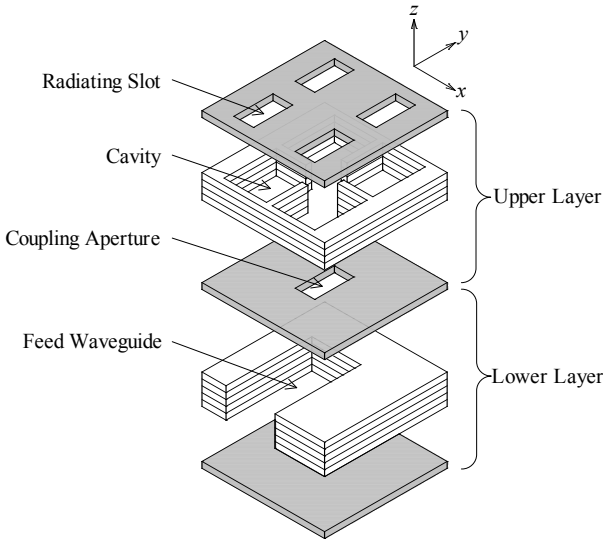

Fig. 2. Explored perspective view of the 2×2-element subarray

2.2 Design

The 2×2-element subarray is a design unit of the proposed antenna. Fig. 3 shows the model of the 2×2-element subarray to analyze the frequency characteristic of the reflection to the feed waveguide. Two sets of periodic boundary walls are placed in the external region to simulate the mutual coupling in the infinite two-dimensional slot array.

The design frequency of the antenna is 61.5 GHz, and

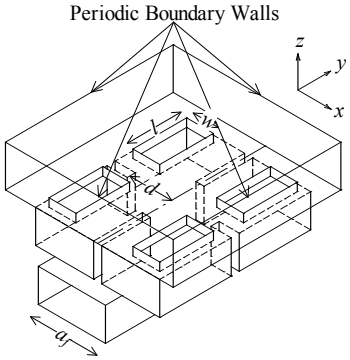

Fig. 3. Analysis model of the 2×2*-element subarray*

the slot spacing in the *x* and *y* directions are fixed to be $4.2\,\text{mm}$ (0.86 wavelengths at the design frequency). The model was analyzed by using Ansoft HFSS and the goal was to optimize the design parameters as much as possible to achieve a simple design. Here, they are the length l and the width w of the slot, the width a_f of the feed waveguide and the distance d between the cavity center and the wall edge in the x direction as shown in Fig. 3. A wideband reflection characteristic with double-tuned impedance matching is achieved in the 2×2-element subarray with the periodic boundary walls for various aspect ratios w/l.

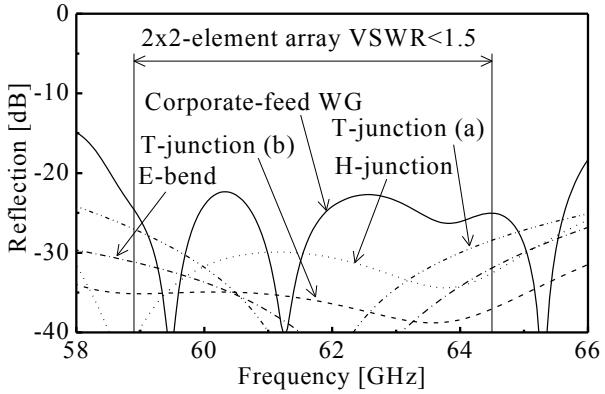

Fig. 4. Reflection coefficient at each port.

The full-corporate-feed waveguide for the 16×16-element array antenna consists of an E-bend, four T-junctions and an H-junction from the feed aperture to the coupling aperture. In order to suppress the reflection from the array antenna over a wide bandwidth, the reflection bandwidth of each part should be extended. Fig. 4 shows the frequency characteristics of the reflection coefficient of each part. The design of the E-bend is shown in the beginning and its reflection characteristic is below $-31\,\text{dB}$ over the bandwidth of interest for VSWR < 1.5 in the 2×2-element subarray.

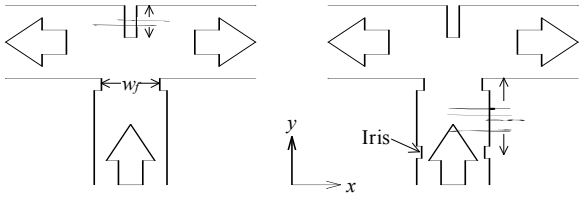

Fig. 5. H-plane T-junction. (a) T-junction without iris. (b) T-junction with iris

The design of each of the first four H-plane T-junctions from the feed aperture is shown in Fig. 5. These first four T-junctions are far enough from each other so that they do not to couple with higher modes and they can be designed independently. The reflection of a conventional T-junction, (a) shown in Fig.5, is below -27 dB over the bandwidth for VSWR < 1.5 in the 2×2-element subarray. However, this reflection is not enough for the full-corporate-feed circuit. Therefore, an iris is installed at a distance of a quarter of the guided wavelength away from the window. The reflections from the window and the iris are cancelled with each other since the round-trip phase difference is 180 degrees. As a result, the reflection of the T-junction, (b) shown in Fig. 5, with the iris is below $-35\,\text{dB}$ over the same bandwidth.

Finally, the design of the H-plane H-junction should be considered. Since the two T-junctions are so close to each other that their higher modes couple to each other. Because of that they should be designed as one body by including the higher modes. The reflection of the H-junction is below $-30\,\text{dB}$ over the bandwidth for VSWR < 1.5 in the 2×2-element subarray as shown in Fig. 4. The amplitude and phase variation among the four output ports are 0.1 dB and 1.4 degrees in the H-junction, respectively. The wideband full-corporate-feed waveguide for the 16×16-element array antenna is designed to excite all the coupling apertures uniformly, both in amplitude and phase. The reflection is below $-20\,\text{dB}$ in 11.8% bandwidth, and it is below $-22.3\,\text{dB}$ over the VSWR < 1.5 bandwidth in the 2×2-element subarray. The amplitude and phase variation over this bandwidth are $0.4\,\text{dB}$ and 3.6 degrees among all the coupling apertures, respectively.

The full structure of the 16×16-element array antenna that combines the 2×2-element subarrays and the full-corporate-feed waveguide is analyzed by HFSS. Fig. 6 shows the frequency characteristic of the reflection at the feed aperture. The bandwidth for VSWR < 1.5 is 8.3% ($58.8\,\text{GHz}$ – $63.9\,\text{GHz}$) that is narrower than 9.1% in the 2×2-element subarray with the periodic boundary walls due to the ripples around $64\,\text{GHz}$. There are two differences between the two models. One is in terms of the pe-

riodic boundary walls and the other is in terms of the full-corporate-feed waveguide. The ripples come from the reflection from the full-corporate-feed waveguide, because similar ripples appear in the reflection of the 16×16-element array antenna if it is analyzed by assuming the periodic boundary walls around the periphery as shown in Fig. 6.

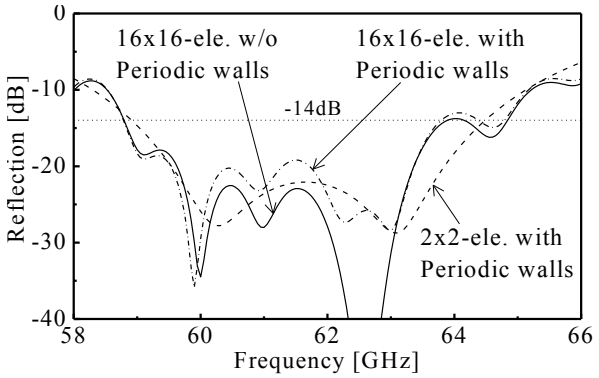

Fig. 6. Reflection coefficient of the 16×16*-element array*

2.3 Experimental Results

The 16×16-element array antenna in the 60 GHz-band is fabricated by diffusion bonding of laminated thin metal plates ($75 \times 76\,\text{mm}^2$ or 15.4 wavelengths $\times$ 15.6 wavelengths at 61.5 GHz). Fig. 7 shows the picture of the fabricated antenna. The aperture area is defined as 67.2 mm (= 16 elements $\times$ 4.2 mm spacing) square. Each of the slot layers has 0.3 mm thickness, the cavity layer is 1.2 mm thick, the coupling aperture layer is 0.3 mm thick and the feed waveguide layer is 1.2 mm thick and they are composed by laminating thin copper plates with 0.3 mm thickness. The 6.0 mm thickness for the feed aperture is not required for the antenna operation. It is installed just to connect a standard WR15 waveguide by screws for the measurement.

Fig. 8 shows the frequency characteristic of the reflection at the feed aperture. The solid line with some width shows the measured reflection including the deviation among eight fabricated antennas. The measured reflection is degraded but it is below -12.6 dB over the bandwidth for the calculated VSWR < 1.5. The measured frequency characteristic is shifted for about 600 MHz lower than the calculated one. In order to identify the factors for the shift, we have done calculations for various values of over-etching. The result assuming 0.02 mm over-etching for all the layer patterns is added into Fig. 8, which agrees with the measured result in the whole bandwidth; we can conclude that the difference between the original calculation and the measurement comes from over-etching by 0.02 mm. The reflection coefficient is very sensitive to this fabrication error, but we have confirmed that other characteristics such as radiation patterns, gain and efficiency are stable and almost unchanged.

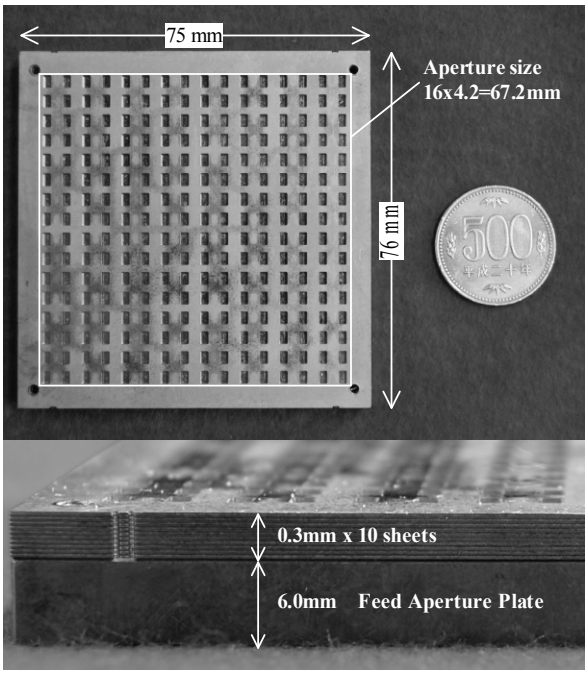

Fig. 7. Picture of the linearly-polarized antenna

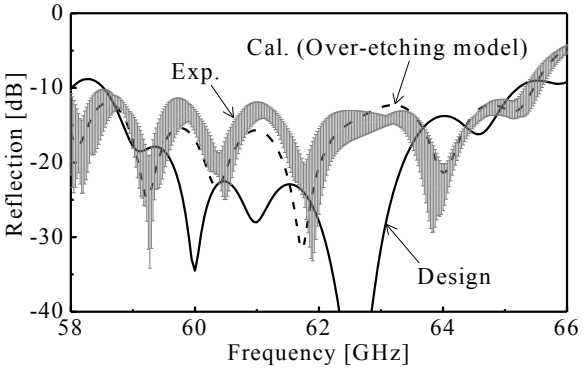

Fig. 8. Frequency behavior of reflection coefficient

The radiation patterns at 62 GHz are measured in the E-(xz) plane and the H-(yz) plane. Good agreement is observed between the measured pattern and the calculated one. In the E-plane, the measured first sidelobe level is -15 dB and it is slightly lower than the calculated one (-13 dB). The measured H-plane pattern coincides with ideal one that was obtained from uniform illumination and it is shown in Fig. 9. The 3 dB-down beamwidth in both the E and H-planes is 3.8 degrees. The measured cross-polarization level is well suppressed below -45 dB in both

planes even though the slots are wide.

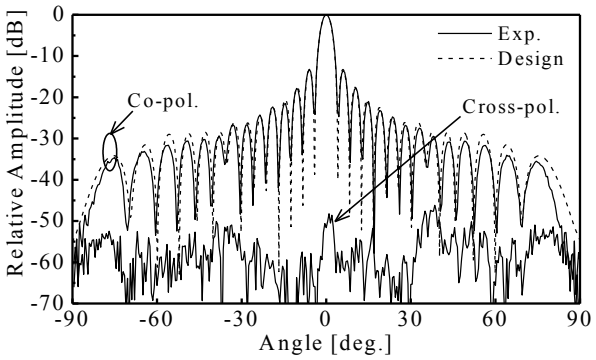

Fig. 9. H-plane radiation pattern

Fig. 10 shows the frequency behavior of the directivity, gain and efficiency characteristics. The measured directivity is calculated by Fourier transforming the near-field distribution. The gain of the eight fabricated antennas is measured in an anechoic chamber and compared with a standard gain horn. The conductor loss and the reflection loss are included in the gain. The solid area indicates the measured gain including the deviation among the eight antennas, which is well predicted by the calculation. The measured directivity is 33.5 dBi at the design frequency (61.5 GHz) and the aperture efficiency is 93.7%. High antenna efficiency of 83.6% is achieved by measuring antenna gain of 33 dBi including the losses. The measured 1 dB-down bandwidth of the gain is 11% (the full-corporate-feed was present).

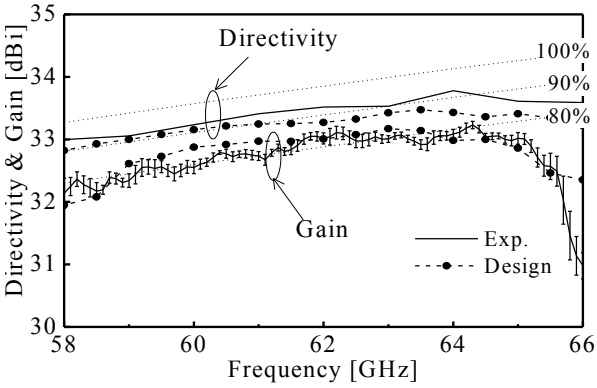

Fig. 10. Frequency behavior of directivity, gain and efficiency

3 CIRCULARLY-POLARIZED ANTENNA

3.1 Structure and Design

Fig. 11 shows a 2 × 2-element subarray of hexagonal radiating apertures that have truncated corners. There is a radiating aperture on each exciting slot as shown in the figure. The propagation of the higher-order coupling modes in the exciting slot region is suppressed by enlarging the attenuation constant with a narrow exciting slot. The dimensions *a* and *c* of the hexagonal radiating aperture are chosen so that only the E_a-polarized and E_b-polarized modes propagate. The wave excited by the exciting slot is decomposed into the E_a-polarized and E_b-polarized modes in the radiating aperture. These two modes propagate with different phase constants. The phase of the Ea-polarized mode advances more than that of the E_b-polarized mode because the phase constant of the E_a-polarized mode is smaller than that of the E_b-polarized mode. The synthesized field must be designed to become a perfectly circular polarized wave by exciting the orthogonal E_a-polarized and E_b-polarized modes with the same amplitude and the phase difference of 90 degrees.

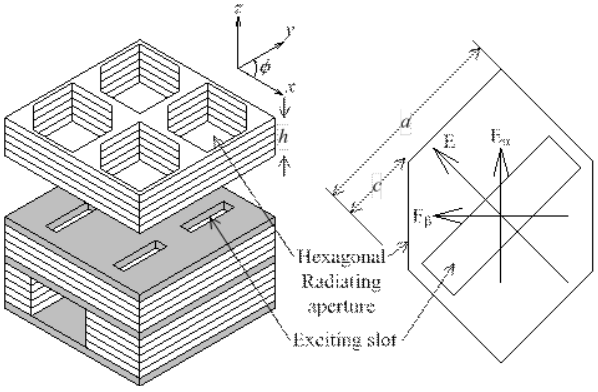

Fig. 11. Configuration of the circularly-polarized element

The circularly-polarized elements are designed at 61.5 GHz by Ansoft HFSS, and the frequency characteristics of the axial ratio at the boresight are compared. The model for the analysis consists of two parts: the exciting slot and the circularly-polarized element as shown on the right side in Fig. 11. The dominant mode is excited directly by the exciting slot. Two sets of periodic boundary walls are placed in the outside region to simulate the mutual coupling in an infinite two-dimensional array of elements. The element spacing in the *x* and *y* directions are fixed to be 4.2 mm which is 0.86 wavelengths at the design frequency.

The exciting slot for the hexagonal aperture models in Fig. 11 is 2.5 mm long, which is about half the wavelength, and is 0.4 mm wide. The thickness of the exciting slot is 0.3 mm. It was confirmed that the grating-lobe level of the array antenna in the $\phi = 45$ degree cut plane is less than -40 dB. The design parameters for the hexagonal aperture are *a* and *c*, and those for the rectangular aperture are *l* and *w*. The minimum height of the hexagonal radiating aperture is 3.0 mm, sufficient to obtain perfectly circular po-

larization. For this height, a is 3.56 mm, c is 1.37 mm, l is 3.5 mm, and w is 2.69 mm.

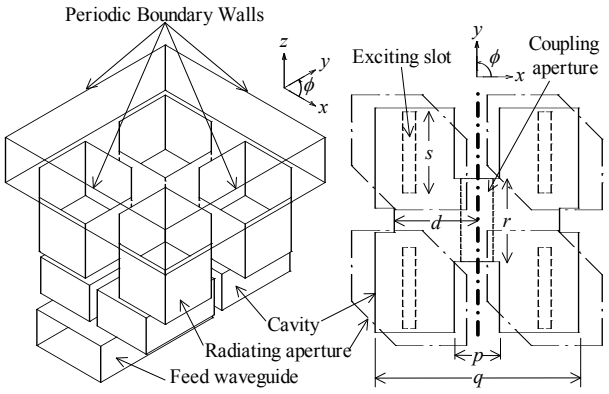

Fig. 12. Model for the analysis of the 2×2*-element subarray*

Fig. 12 shows the model of the 2×2-element subarray used to analyze the frequency characteristics of the reflection to the feed waveguide. The parameters to suppress the reflection are the length s of the exciting slot, the width q of the cavity, the distance d between the cavity center and the wall edge in the x direction, the width p of the wall in the y direction in the cavity, and the length r of the coupling aperture as shown in Fig. 12. The distance between the two walls in the y direction is equal to r.

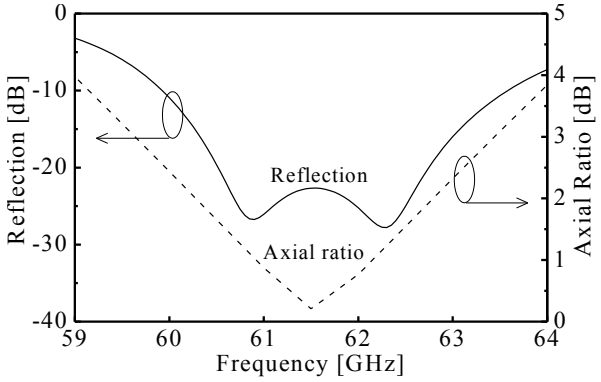

Fig. 13. Reflection coefficient and axial ratio of the 2×2*-element subarray*

Fig. 13 shows the frequency characteristics of the reflection and the axial ratio. The overall reflection at the feed aperture can be realized as less than -14 dB when combined with a 64-way power divider for a 16×16-element array with a -30 dB reflection. The bandwidth for VSWR < 1.5 is 4.8% and the local maximum value of the reflection is -22.7 dB. The bandwidth of the axial ratio (when below 3 dB) is 6.2%, and it is below 2.5 dB over the bandwidth for VSWR < 1.5. In the sensitivity simulation of the position error of the radiating aperture, the maximum variation of the axial ratio is found to be only 0.18 dB within an error range of ± 0.2 mm in the x and y directions.

3.2 Experimental Results

A 16×16-element array antenna that combines 64 2×2-element subarrays and a 64-way divider was fabricated by diffusion bonding of laminated thin metal plates in the 60 GHz-band. Fig. 14 shows the picture of the fabricated antenna. The size is 75×76 mm^2 (15.4 wavelengths $\times$ 15.6 wavelengths at 61.5 GHz), and the aperture area is a 67.2 mm^2. The radiating aperture layer, the exciting slot layer, the cavity layer, the coupling aperture layer, and the feed waveguide layer are formed by laminating 0.3 mm thick copper plates. The bottom 6.0 mm thick plate for the feed aperture is not involved in the antenna operation, but has been added to connect the antenna to a standard WR15 waveguide by screws for the measurements.

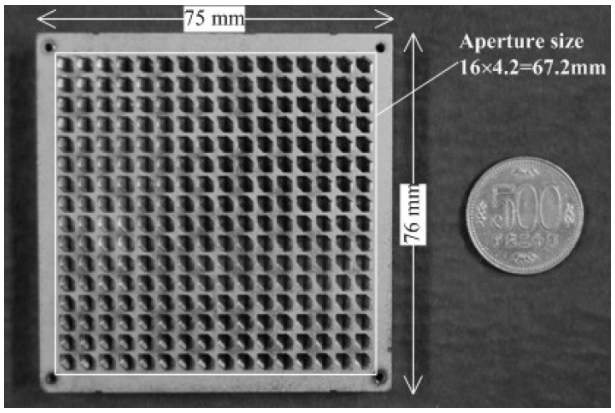

Fig. 14. Picture of the circularly-polarized antenna

The measured reflection didn't not agree with the calculated reflection. To identify the reasons for this degradation, results with different values of over-etching were calculated. The result assuming a 0.03 mm over-etching across the layer patterns agreed very well with the measured result over the full bandwidth.

The spin-linear radiation patterns were measured at 61.5 GHz. Fig. 15 shows the patterns in the $\phi = 0$ and 90 degree cut planes. The pattern in the $\phi = 0$ deg. cut plane has grating-lobes of about -20 dB, reflecting the ripples in the amplitude distribution in the x direction. The pattern in the $\phi = 90$ deg. cut plane coincides well with that obtained from a uniform illumination. The axial ratio is about 1 dB in the main beam.

Fig. 16 shows the frequency characteristic of the axial ratio. The measured frequency bandwidth when axial ratio is less than 3 dB is 4.3%. The measured frequency

characteristic is shifted for about 500 MHz lower than the calculated characteristics, and shows that the axial ratio is degraded for 0.6 dB. However, this does not agree with the calculation assuming 0.03 mm over-etching. The reason for this discrepancy is now under investigation.

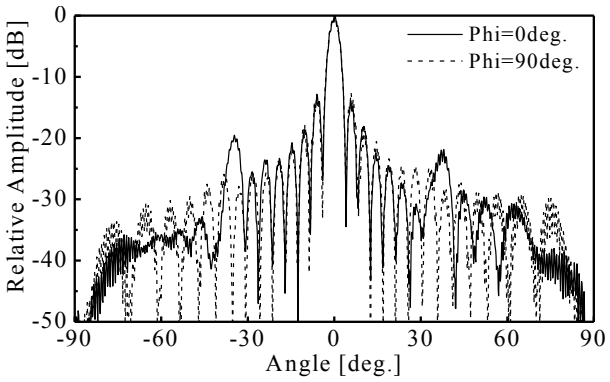

Fig. 15. Radiation patterns

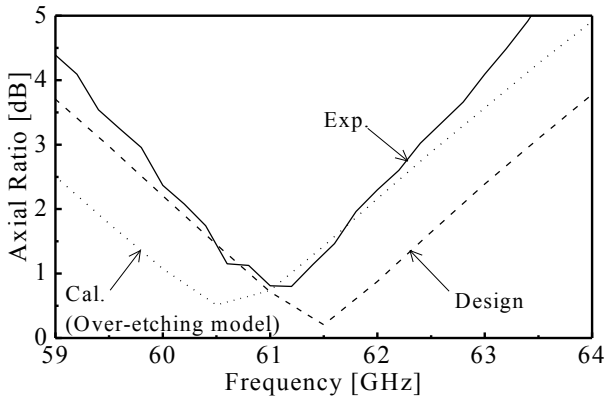

Fig. 16. Axial ratio characteristics of the 16×16*-element array*

Fig. 17 shows the frequency behavior of the gain measured in an anechoic chamber with the antenna efficiency including the losses. The gain measurements compare the receiving level of the fabricated antenna with a standard horn antenna with a known gain of about 25 dBi. In the measurements with the fabricated antenna, the receiving horn antenna rotates slowly to measure the axial ratio of the fabricated antenna. The measured axial ratio is included to correct the circularly-polarized gain of the fabricated antenna The measured gain does not agree with the calculated gain, however it is well predicted by the calculations assuming 0.03 mm over-etching. The gain around 63 GHz is degraded due to reflection loss. A high antenna efficiency of 91.6% is achieved by measuring the antenna gain of 33.4 dBic at the design frequency of 61.5 GHz. The measured 1 dB-down gain bandwidth is 4.4%.

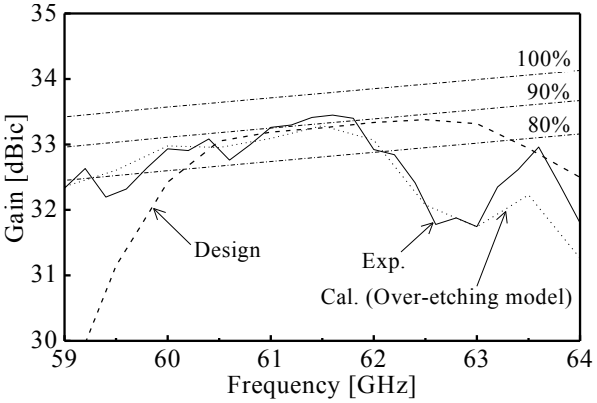

Fig. 17. Frequency behavior of gain and antenna efficiency

4 TILTED-LINEARLY-POLARIZED ANTENNA

4.1 Structure and Design

Fig. 18 shows the exploded perspective view of the 2×2-element sub-array as the radiation unit. Four exciting slots are placed on a cavity to excite 45-degree inclined radiating slots. The number of required etching patterns for fabrication by diffusion bonding is six: the radiating slots, exciting slots, cavities, coupling apertures, feeding circuit, and feeding aperture.

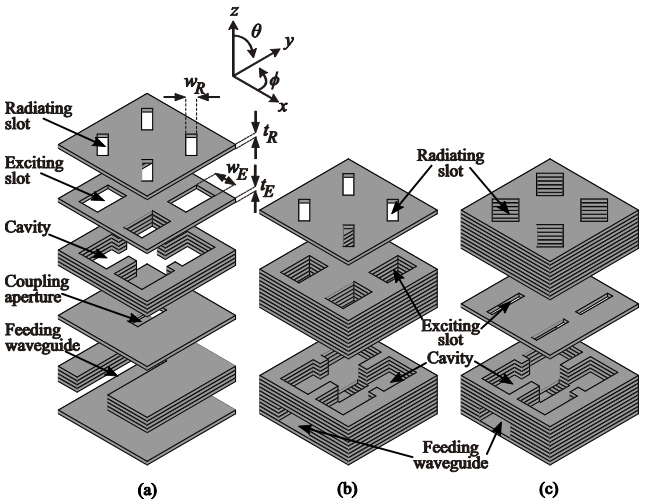

Fig. 18. Exploded perspective view of the 2×2*-element array. (a) Initial model, (b) The thick exciting slot model, (c) The narrow exciting slot model*

In the analysis, two pairs of periodic boundary walls were assumed to calculate mutual coupling among the sub-arrays in an infinite two-dimensional array. The design frequency was 61.5 GHz, and the slot spacing in the *x*- and *y*-directions was fixed to 4.2 mm ($0.86\lambda_0$ at the design frequency). This model was analyzed by Ansoft HFSS. The

design is constructed as follows. At first, the dimension of the exciting slots is adjusted to realize uniform excitation of the radiating slots. Next, the dimension of the radiating slots is determined to suppress cross-polarization. Finally, the dimensions of the cavity and the coupling aperture are controlled to match the impedance with the feeding waveguide.

To realize a uniform excitation, the electromagnetic field in the cavity has to be symmetric. One way to achieve this is through the propagation of the dominant mode and ensuring that the higher-order modes are in cut-off for the exciting slots. Therefore, the exciting slots have to be thick or narrow enough since the attenuation E and its constant α of TEmn modes through the exciting slots are expressed by

$$E = E_0 \exp\left(-\alpha t_E\right), \tag{1}$$

$$\alpha = \sqrt{\left(\frac{m\pi}{l_E}\right)^2 + \left(\frac{n\pi}{w_E}\right)^2 - k^2}, \tag{2}$$

where t_E, l_E and w_E are the thickness, length, and width of the exciting slots, respectively, and k is the wave number in free space.

To suppress the higher-order modes and excite all the radiating slots uniformly, the exciting slots have to be thick or narrow enough, as shown in Fig. 18 (b) and (c). Two different ways to suppress cross-polarization are considered for each, the thick and the narrow exciting slot models. For the thick exciting slot model shown in Fig. 18 (b), the cross-polarization is suppressed by the radiation slot width *wR*, as shown in Fig. 19. For the narrow exciting slot model illustrated in Fig. 18 (c), the radiating slots have to be wide enough to be excited. Otherwise, the radiating slots are not excited and no electromagnetic wave is radiated. Hence, wide slots are adopted as the radiating elements for the narrow exciting slot model and cross-polarization is suppressed by the thickness of the radiating slots *tR*, as shown in Fig. 19. The principle of cross-polarization suppression is the same as the higher-order mode suppression, as stated in the above paragraph.

Therefore, two configurations can be obtained for uniform excitation and low cross-polarization: the thick exciting slot model and the narrow exciting slot model, as shown in Fig. 18 (b) and (c). The thick exciting slot model is composed of thick exciting slots and narrow radiating slots. The narrow exciting slot model is composed of narrow exciting slots and thick radiating slots.

Finally, the impedance is matched with the feeding waveguide by adjusting the length and width of the walls in the cavity and the length of the coupling aperture. The frequency characteristic of the reflection coefficient is shown in Fig. 20. The bandwidth for VSWR less than 1.5 is 3.1% and 7.2% for the thick exciting slot model and narrow exciting slot model, respectively.

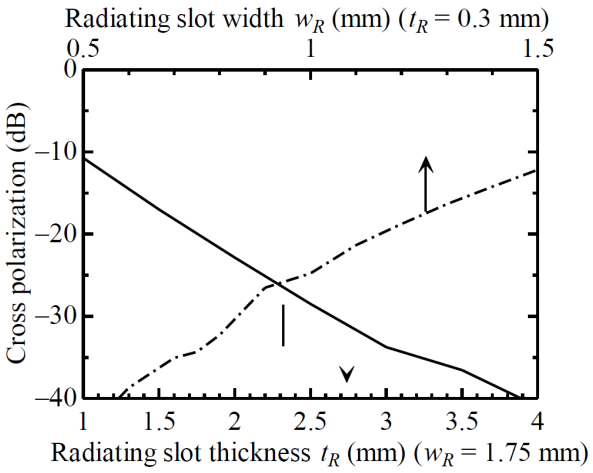

Fig. 19. Cross-polarization suppression by the radiating slot width and the radiating slot thickness

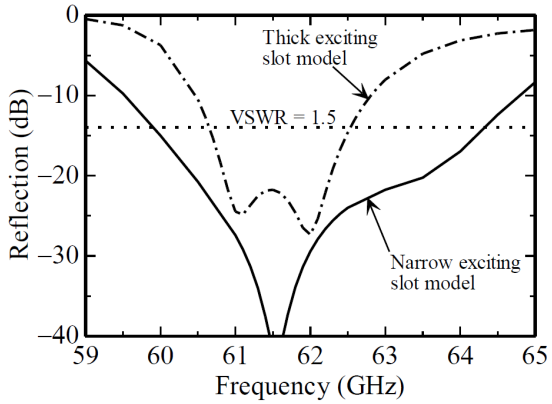

Fig. 20. Reflection coefficient of the 2 × 2-element subarrays

4.2 Experimental results

The designed 16 × 16-element array was fabricated by the diffusion bonding of the laminated thin copper plates. The dimension of each plate was 75 mm × 76 mm × 0.3 mm. The picture of the fabricated antenna is shown in Fig. 21. The total thickness is 6.6 mm, composed of 3 mm for the radiating slot, 0.3 mm for the exciting slots, 1.2 mm for the cavities, 0.3 mm for the coupling aperture, 1.2 mm for the feeding waveguides, and 0.6 mm for the feeding aperture. As all elements are formed by etching, under- and over-etching may occur.

The measured reflection characteristic was degraded and was shifted to the lower band. The shift to the lower frequency may be caused by over-etching. To identify the over-etching amount, 16 × 16-element array models with several over-etching amounts were simulated. The simulated reflection of the 0.03 mm over-etching model

agrees well with the measured result. Hence, the difference between the measurement and simulation comes from the 0.03 mm over-etching. Although over-etching affects the reflection characteristics, the simulations and measurements have confirmed that radiation characteristics, such as radiation patterns, cross-polarization, and directivity, are stable.

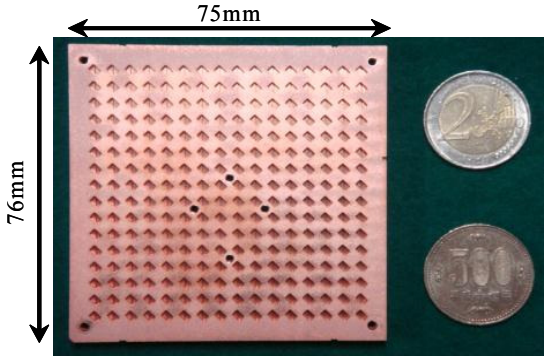

Fig. 21. Picture of the tilted-linearly-polarized antenna

Fig. 22 shows the measured and simulated radiation patterns at 61.5 GHz in the *E*-plane ($\phi = 45$ deg.), and $\phi = 0$ deg. plane. In the *E*- and *H*-plane, both the measured and simulated patterns agree with each other very well. The measured first sidelobe levels in the *E*- and *H*-plane are -25.5 dB and -26.1 dB, respectively. However, in the $\phi = 0$-degree plane, -21.8 dB grating lobes are observed at $\theta = \pm 35$ degree directions because of the rippled amplitude distribution in the *x*-axis direction. The rippled amplitude distribution and the grating lobes are caused by the misalignment of the exciting slot position in the *x*-axis direction. We assume that the four exciting slots shift in the *x*-axis direction. Two of them approach the sidewall of the cavity and couple more strongly with the magnetic field in the cavity. In contrast, the others become apart from the sidewall of the cavity and the coupling becomes weak. The 16×16-arrays with several exciting slot shift distances were simulated. The radiation pattern of the 0.04 mm shift is also shown in Fig. 22 (b). The grating lobes in the ± 35 degree directions agree well. Therefore, we can conclude that the rippled amplitude in the *x*-axis direction and the corresponding grating lobes result from the shift of the exciting slots. The simulations show that the reflection characteristic is not affected much by the exciting slot shift.

The frequency characteristic of the measured and simulated cross-polarization is shown in Fig. 23. The measured result agrees with the simulated one, and -31.7 dB is obtained at the design frequency. The measured gain and directivity are shown in Fig. 23 with the simulated results. The gain is measured by comparison with a standard gain horn in an anechoic chamber and it includes the reflection loss. The directivity is calculated from the measured near-field distribution by Fourier transform. The measured gain is degraded compared to the simulated one because of the reflection loss. However, antenna efficiency greater than 70% is achieved over 5 GHz bandwidth, and 33.0 dBi gain is realized at the design frequency. The same measured gain with [18] was obtained, even though the proposed antenna has additional loss: polarization conversion loss and conductor loss of the additional layer. The reason is that all of the losses are negligible: the polarization loss is 0.003 dB and the estimated conductor loss is 0.016 dB. The measured directivity is degraded around the center frequency relative to the simulated one. The directivity at the design frequency is 33.3 dBi and the corresponding aperture efficiency is 88.7%.

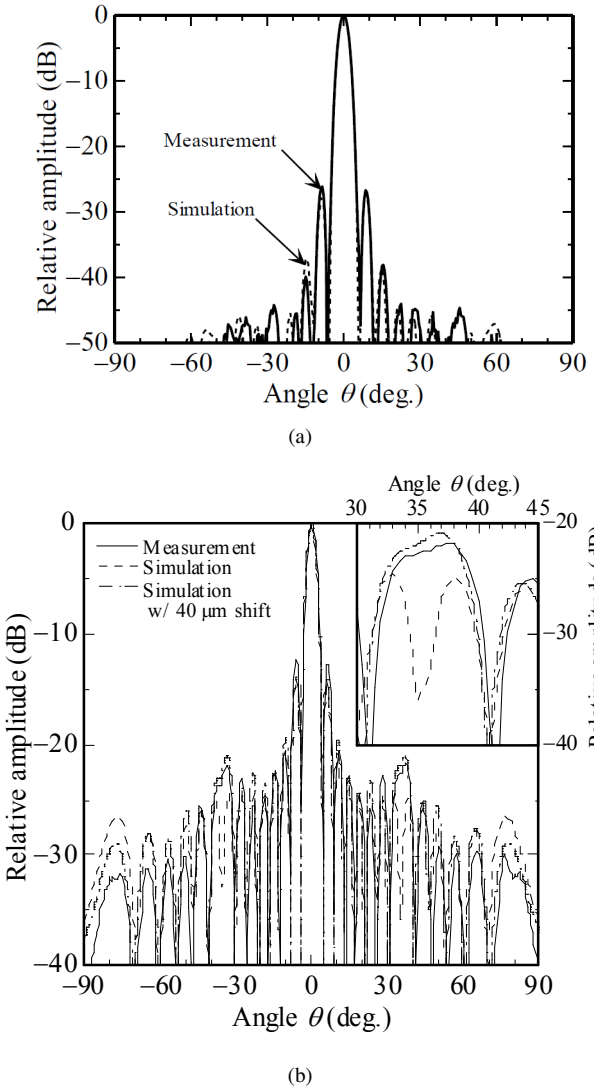

Fig. 22. Radiation pattern at 61.5 *GHz. (a) E-plane (*$\phi = 45$ *deg.), (b)* $\phi = 0$ *deg. plane*

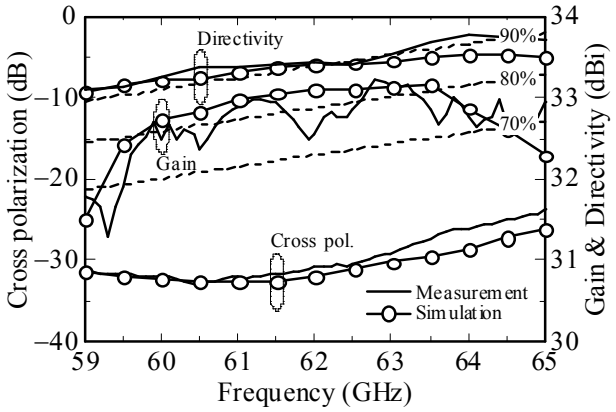

Fig. 23. Frequency characteristic of cross-polarization, gain, and directivity

5 CONCLUSION

This paper has reviewed the plate-laminated waveguide slot array antennas and their polarization conversion layers. Diffusion bonding of thin metal plates to make multi-layer hollow corporate-feed waveguide structures has given high antenna efficiency of about 80% over a wide bandwidth in 16×16-element array antennas in the 60 GHz band. An additional layer to convert to circular or tilted-linear polarizations keeps the good antenna performances.

REFERENCES

[1] E. Levine, G. Malamud, placeS. Shtrikman, and D. Treves, "A study of microstrip array antennas with the feed network," IEEE Trans. Antennas Propag. vol.37, no. 4, pp.426-434, Apr. 1989.

[2] R. C. Johnson, and H. Jasik, Antenna Engineering Handbook, McGraw-Hill, Chap.9, 1984.

[3] S. S. Oh, J. W. Lee, M. S. Song and Y. S. Kim, "Two-layer slotted-waveguide antenna array with broad reflection/gain bandwidth at millimetre-wave frequencies," IEE Proc.-Microw. Antennas Propag., vol.51, no. 5, pp.393-398, Oct. 2004.

[4] Y.Miura, J.Hirokawa, M.Ando, Y.Shibuya and G.Yoshida, "Double-layer full-corporate-feed hollow-waveguide slot array antenna in the 60GHz-band," IEEE Trans. Antennas Propagat., vol.59, no.8, pp.1521-1527, Aug. 2011.

[5] J. Hirokawa, M. Zhang, and M. Ando, "94GHz single-layer slotted waveguide array by diffusion bonding of laminated thin plates," 2008 Intl. Symp. Antennas Propagat., TP-C03-3, Oct. 2008.

[6] K. Jung, H. Lee, G. Kang, S. Han and B. Lee, "Cavity-backed planar slot array antenna with a single waveguide-fed sub-array," 2004 IEEE AP-S Int. Symp., 115.5, Jun. 2004.

[7] B. Lee, K. Jung and S. Yang, "High-efficiency planar slot array antenna with a single waveguide-fed cavity-backed subarray," Microwave and Optical Technology Letters, vol.43, no. 3, pp.228-231, Nov. 2004.

[8] N. Yoneda, M. Miyazaki, H. Matsumura, and M. Yamato, "A design of novel grooved circular waveguide polarizers," IEEE Trans. Microwave Theory Technique, MTT-48, pp. 2446-2452, Dec. 2000.

[9] Y. Aramaki, H. Uchida, T. Nishino, N. Yoneda, I. Naito, H. Miyashita, and Y. Konishi, "COP millimeter-wave horn array antenna," 2008 Intl. Symp. Antennas Propagat., pp. 37-40, Oct. 2008.

[10] T. Tsugawa, Y. Sugio, and Y. Yamada, "Circularly polarized dielectric-loaded planar antenna excited by the parallel feeding waveguide network," IEEE Trans. Broadcasting, vol.43, no.2, pp.205-212, Jun. 1997.

[11] Y.Miura, J.Hirokawa, M.Ando, K.Igarashi and G.Yoshida, "A high-efficiency circularly-polarized aperture array antenna with a corporate-feed circuit in the 60GHz band," IEICE Trans. Electron., vol.94, no.10, pp.1618-1625, Oct. 2011.

[12] T. Murata, H. Mitsumoto, M. Fujita, S. Tanaka, K. Takano, K. Imai, and N. Toyama, "Portable digital satellite news gathering (SNG) RF terminal using a flat antenna," IEICE Trans. Commun., vol.E77-B, no.12, pp.1501-1510, Dec. 1994.

[13] M. Sato, Y. Konishi, and S. Urasaki, "A travelling-wave fed parallel plate slot array antenna with inclined linear polarisation at 60GHz," IEICE Tech. Rept., AP96-127, Jan. 1997.

[14] J. Hirokawa, and M. Ando, "45-deg linearly polarized post wall waveguide-fed parallel plate slot arrays," IEE Proc., Microw. Antennas Propag., vol.147, pp.515-519, Dec. 2000.

[15] K. Sakakibara, T. Watanabe, K. Sato, K. Nishikawa, and K. Seo, "Millimeter-wave slotted waveguide array antenna manufactured by metal injection molding for automotive radar systems," IEICE Trans. Commun., vol.84, no.9, pp.2369-2376, Sept. 2001.

[16] H. Iizuka, T. Watanabe, K. Sato, and K. Nishikawa, "Millimeter-wave microstrip array antenna for automotive radars," IEICE Trans. Commun., vol.86, no.9, pp.2728-2738 Sept. 2003.

[17] T.Tomura, Y.Miura, M.Zhang, J.Hirokawa and M.Ando, "Design of a 45-degree linearly-polarized hollow-waveguide slot two-dimensional array antenna with a full-corporate-feed circuit in the lower layer," 2010 Intl. Symp. Antennas Propagat., TC3.2, Nov.2010.

[18] M. Zhang, J. Hirokawa, and M. Ando, "Design of a partially-corporate feed double-layer slotted waveguide array antenna in 39 GHz band and fabrication by diffusion bonding of laminated thin metal plates," IEICE Trans. Commun., vol.93, no.10, pp. 2538-2544, Oct. 2010.

Jiro Hirokawa was born in Tokyo, Japan, on May 8, 1965. He received the B.S., M.S. and D.E. degrees in electrical and electronic engineering from Tokyo Institute of Technology (Tokyo Tech), Tokyo, Japan in 1988, 1990 and 1994, respectively. He was a Research Associate from 1990 to 1996, and is currently an Associate Professor at Tokyo Tech. From 1994 to 1995, he was with the antenna group of Chalmers University of Technology, Gothenburg, Sweden, as a Postdoctoral Fellow. His research area has been in slotted waveguide array antennas and millimeter-wave antennas. He received an IEEE AP-S Tokyo Chapter Young Engineer Award in 1991, a Young Engineer Award from IEICE in 1996, a Tokyo Tech Award for Challenging Research in 2003, a Young Scientists' Prize from the Minister of Education, Cultures, Sports, Science and Technology in Japan in 2005, a Best Paper Award in 2007, a Best Letter Award in 2009 from IEICE Communications Society and Asia Pacific Microwave Conference prize in 2011. He is a Fellow of IEEE and a Senior Member of IEICE.

AUTHORS' ADDRESSES

Assoc. Prof. Jiro Hirokawa, Ph.D.
Department of Electrical and Electronic Engineering,
Tokyo Institute of Technology,
S-20, 2-12-1 Ookayama, Meguro-ku, Tokyo 152-8552,
Japan
email: jiro@antenna.ee.titech.ac.jp

Received: 2011-12-16
Accepted: 2012-01-23